CKIP-1 regulates mammalian and zebrafish myoblast fusion

Dominique Baas[1,], Sabine Caussanel-Boude[1,*,**], Alexandre Guiraud[1,**], Frederico Calhabeu[1,‡,**], Emilie Delaune[1], Fanny Pilot[1,§], Emilie Chopin[1,¶], Irma Machuca-Gayet[2], Aurélia Vernay[1], Stéphanie Bertrand[3], Jean-François Rual[4], Pierre Jurdic[2], David E. Hill[4], Marc Vidal[4], Laurent Schaeffer[1,**] and Evelyne Goillot[1,**,‡‡]**

[1]Equipe Différenciation Neuromusculaire, Laboratoire de Biologie Moléculaire de la Cellule, CNRS UMR 5239/ENS Lyon, Université de Lyon, IFR128 Biosciences Lyon-Gerland, 46 Allée d'Italie, 69364 LYON cedex 07, France
[2]Équipe Biologie Cellulaire et Physiopathologie Osseuse, Institut de Génomique Fonctionnelle de Lyon (IGFL) UMR 5242 CNRS - ENS Lyon - INRA 1288 - UCB Lyon 1, 46 Allée d'Italie, 69364 LYON cedex 07, France
[3]CNRS UMR 7628, UPMC Université Paris 06, Observatoire Océanographique, F-66651 Banyuls-sur-Mer, France
[4]Center for Cancer Systems Biology and Department of Cancer Biology, Dana-Farber Cancer Institute and Department of Genetics, Harvard Medical School, Boston, MA 02115, USA

*Present address: Faculté de médecine Lyon-RTH Laennec de l'Université Claude Bernard Lyon 1, 69622 Villeurbanne cedex, France
‡Present address: Randall Division of Cell and Molecular Biophysics, King's College London, Guy's Campus, London, UK
§Present address: UMR 955 INRA-ENVA de Génétique Moléculaire et Cellulaire, 7 Avenue Général de Gaulle, 94700 Maisons-Alfort, France
¶Present address: Equipe Contrôle de l'Expression Génétique et Oncogenèse Virale, Laboratoire de Biologie Moléculaire et Cellulaire, CNRS UMR 5239/ENS Lyon, Université de Lyon, IFR128 Biosciences Lyon-Gerland, 46 Allée d'Italie, 69364 LYON cedex 07, France
**These authors contributed equally to this work
‡‡Author for correspondence (evelyne.goillot@ens-lyon.fr)

Accepted 2 April 2012
Journal of Cell Science 125, 3790–3800

doi: 10.1242/jcs.101048

Summary

Multinucleated muscle fibres arise by fusion of precursor cells called myoblasts. We previously showed that CKIP-1 ectopic expression in C2C12 myoblasts increased cell fusion. In this work, we report that CKIP-1 depletion drastically impairs C2C12 myoblast fusion in vitro and in vivo during zebrafish muscle development. Within developing fast-twich myotome, Ckip-1 localises at the periphery of fast precursor cells, closed to the plasma membrane. Unlike wild-type myoblasts that form spatially arrayed multinucleated fast myofibres, Ckip-1-deficient myoblasts show a drastic reduction in fusion capacity. A search for CKIP-1 binding partners identified the ARPC1 subunit of Arp2/3 actin nucleation complex essential for myoblast fusion. We demonstrate that CKIP-1, through binding to plasma membrane phosphoinositides via its PH domain, regulates cell morphology and lamellipodia formation by recruiting the Arp2/3 complex at the plasma membrane. These results establish CKIP-1 as a regulator of cortical actin that recruits the Arp2/3 complex at the plasma membrane essential for muscle precursor elongation and fusion.

Key words: CKIP-1, Arp2/3, Actin cytoskeleton, Myoblast fusion, Zebrafish muscle development

Introduction

Fusion of myoblasts into syncytial myofibres is a fundamental step in skeletal muscle development in many organisms. In mice, essential fusion events take place during embryogenesis and adult muscle regeneration, and muscle syncytia can eventually reach several hundreds of nuclei in adults. Muscle cell lines such as the established mouse C2C12 line have provided useful models for analysing myoblast fusion. Upon differentiation, C2C12 myoblasts become elongated myocytes, which sequentially migrate, adhere to one another, and fuse to form small nascent myotubes. As myotubes further differentiate, they recruit additional myocytes or myotubes, increasing the number of nuclei in the syncytium, and start expressing contractile proteins (Abmayr and Pavlath, 2012; Rochlin et al., 2010).

In zebrafish embryos, fusion is a key step of fast-twitch myofibres differentiation. Pioneering works have provided a critical knowledge of the cellular events associated with muscle fibre formation in zebrafish. Two distinct lineages of muscle precursors can be distinguished within the zebrafish developing somites (Devoto et al., 1996). The slow-twitch muscle fibres derive from adaxial myogenic precursors which begin to differentiate alongside the notochord while the rest of the myotome gives rise to fast-twitch fibres. The majority of adaxial cells migrate through the lateral myotome, to form the superficial layer of slow muscle. This migration is crucial for zebrafish somite development because it initiates a medial to lateral wave of fast muscle precursor differentiation (Henry and Amacher, 2004). Whereas slow-twitch myoblasts mature into mononucleate fibres, fast muscle precursors fuse with each other to form syncytial myotubes.

Using time-lapse video microscopy of genetic mosaic analysis and mathematical models studies, Snow et al. have provided fundamental insights into the cellular mechanisms that drive fast muscle fibre formation (Snow et al., 2008). They showed that zebrafish fast muscle fibre morphogenesis consists of three phases: short precursor cells with protrusive activity, intercalation/elongation consisting in protrusion extension and filling, boundary capture/myotube formation until both ends of the muscle fibre anchor to the myotendinous junction (boundary capture) and finally fusion. Dynamic interplay between the plasma membrane and the underlying cortical actin cytoskeleton is critical for cell morphogenetic movements leading to fusion. Importantly,

an essential role of actin regulators has been demonstrated in muscle fibre formation in drosophila and mice, and more recently in zebrafish (reviewed in Rochlin et al., 2010).

Filamentous actin is nucleated and organized into branched networks by the actin-related protein 2/3 (Arp2/3 complex), which nucleates new filaments and concomitantly anchors them to the sides of existing filaments, while capping protein (CP) binds to the rapidly growing barbed ends of filaments and terminates their growth (Pollard and Borisy, 2003). Both capping and nucleation activities are tightly coupled and required for dendritic actin networks formation and actin-based motility (Akin and Mullins, 2008; Carlier and Pantaloni, 1997). Nucleation by Arp2/3 complex is activated by a class of proteins termed type I nucleation-promoting factors (NPFs) which bind to the complex and to actin monomers. These NPFs can be associated in complexes with up to six other proteins. These associations combine Arp2/3 activation with additional biochemical functions, including capping protein inhibition (Derivery et al., 2009; Jia et al., 2010).

The pleckstrin homology (PH) domain-containing protein casein kinase 2 interacting protein-1 (CKIP-1) (Bosc et al., 2000) contains a PH domain at the N-terminus and a putative leucine zipper (LZ) motif at the C-terminus. We and others have shown that CKIP-1 is mainly localised at the plasma membrane (Olsten et al., 2004; Safi et al., 2004; Xi et al., 2010) and binds to phosphoinositides through its PH domain (Olsten et al., 2004; Safi et al., 2004; Xi et al., 2010). CKIP-1 interacts with actin capping protein at the barbed ends of actin filaments (Canton et al., 2005; Canton et al., 2006). We previously observed that CKIP-1 ectopic expression in C2C12 myoblasts increases cell fusion (Safi et al., 2004). Consistently, we show in this study that CKIP-1 depletion abolishes C2C12 cell fusion. We examined muscle fibre formation in Ckip-1 antisense morpholino oligonucleotide injected zebrafish embryos and show that Ckip-1 knock down in zebrafish embryo impairs fast-twitch myoblast fusion. Search for CKIP-1 binding partners (Pilot-Storck et al., 2010) identified ARPC1A subunit of Arp2/3 actin nucleation complex. We demonstrate that CKIP-1 regulates cell morphology and lamellipodia formation through membrane recruitment of Arp2/3 complex. These results clearly establish CKIP-1 as a regulator of actin cytoskeleton and suggest a CKIP-1-dependent coordination of Arp2/3 activities. They additionally contribute in vivo functional data to support this hypothesis.

Results

RNA interference-mediated inhibition of CKIP-1 blocks mammalian C2C12 myoblast fusion

To test for a role of CKIP-1 during mammalian myoblast fusion, we inhibited its expression in C2C12 myoblasts by RNA interference. We used two different siRNA targeting CKIP-1 and observed that levels of knock down ranged from approximately 40% to 70% for siRNA1 and siRNA2, respectively, when compared to control siRNA. C2C12 myoblasts were transiently transfected with either CKIP-1-specific siRNAs or scrambled siRNA control that did not affect CKIP-1 expression level together with a GFP-expressing vector. Cells were then switched to differentiation medium for 4 days. As will be shown in supplementary material Fig. S5, CKIP-1 knock down affects cell migration. Because contact between myoblasts is essential for their subsequent fusion and affect cell migration, we minimized any potential influence that inhibition of myoblast migration might exert on the fusion analysis by growing myoblasts to confluence prior to shifting them to differentiation medium. Nuclei number in two to four hundred GFP-positive cells were counted and distributed into five groups according to nuclei number. A representative experiment is shown in (Fig. 1A) and illustrated in Fig. 1C. The corresponding western blot illustrating CKIP-1 inhibition is shown in (Fig. 1B). We found that CKIP-1-knockdown myoblasts failed to fuse normally in comparison to control scrambled siRNA-transfected cells (Fig. 1A). In agreement with CKIP-1 knockdown levels, 62 and 78% of siRNA1 and 2 cells, respectively, remained mononucleated as compared to 35% of scrambled cells. In siRNA-transfected cells the majority of myotubes contained 2 to 5 nuclei. The number of myotubes with more than six nuclei was drastically reduced in these cells (13 and 7% for siRNA1 and 2 cells, respectively) as compared to control cells (36%). The fusion defect of siRNA1 treated cells was almost fully rescued by expression of ectopic CKIP-1 (Fig. 1A–C). The number of mononucleated myoblast was decreased and similar number of myotubes containing 6 to 10, 11 to 15 and more than 15 nuclei were observed in siRNA1 plus wild-type CKIP-1 and scrambled control siRNA-transfected cells (Fig. 1A). The same conclusions were reached in four different experiments represented in Fig. 1D. We previously showed that myogenin expression is slightly delayed CKIP-1 knockdown cells (Safi et al., 2004). Then its expression gets back to normal levels. In order to rule out the possibility of a delayed differentiation due to a weak myogenin expression, we kept the cells in differentiation medium for a longer time and checked the expression of myosin heavy chain, a more tardive marker of differentiation. CKIP-1-depleted myoblasts still expressed sarcomeric myosin heavy chain (MHC), a marker for both mature myotubes and as-yet-unfused terminally differentiated myoblasts (Pajcini et al., 2008; Yoon et al., 2007), indicating that the decreased fusion of treated myoblasts was not due to an inability of these cells to differentiate (Fig. 1E). These results show that CKIP-1n knock down impairs myoblast fusion without interfering with their differentiation program.

Identification of the zebrafish *ckip-1* gene and study of its expression pattern

We then explored CKIP-1 function in zebrafish myogenesis in vivo. For this, we first characterized *ckip-1* gene and its expression pattern in zebrafish embryos. BLAST searches of the Sanger Ensembl zebrafish database identified predicted translation products with significant levels of similarity to the mammalian CKIP-1. A RACE-PCR strategy was devised to amplify the putative zebrafish *ckip-1* cDNA, allowing the recovery of the complete sequence (data not shown). The sequence of the cDNA isolated by this method was found in GenBank under the reference |XP_691398.3| pleckstrin-homology-domain-containing family O member 1-like (*Danio rerio*) GENE ID: 562940 LOC562940. It is predicted to encode a 403 amino acids protein that displays 55.5% identity with mouse CKIP-1 (supplementary material Fig. S1). In its N-terminal part, zebrafish Ckip-1 contains a PH domain (residues 20–131) followed by the CP binding domain (residues 137–165) (Hernandez-Valladares et al., 2010) which display 82 and 89.3% identity with the corresponding mouse domains, respectively. Based on these domains organization and on the quite high level of protein similarity between murine (NP_075809) or human (NP_057358) CKIP-1 and the corresponding zebrafish protein, we concluded that this transcript encodes the zebrafish Ckip-1 homologue.

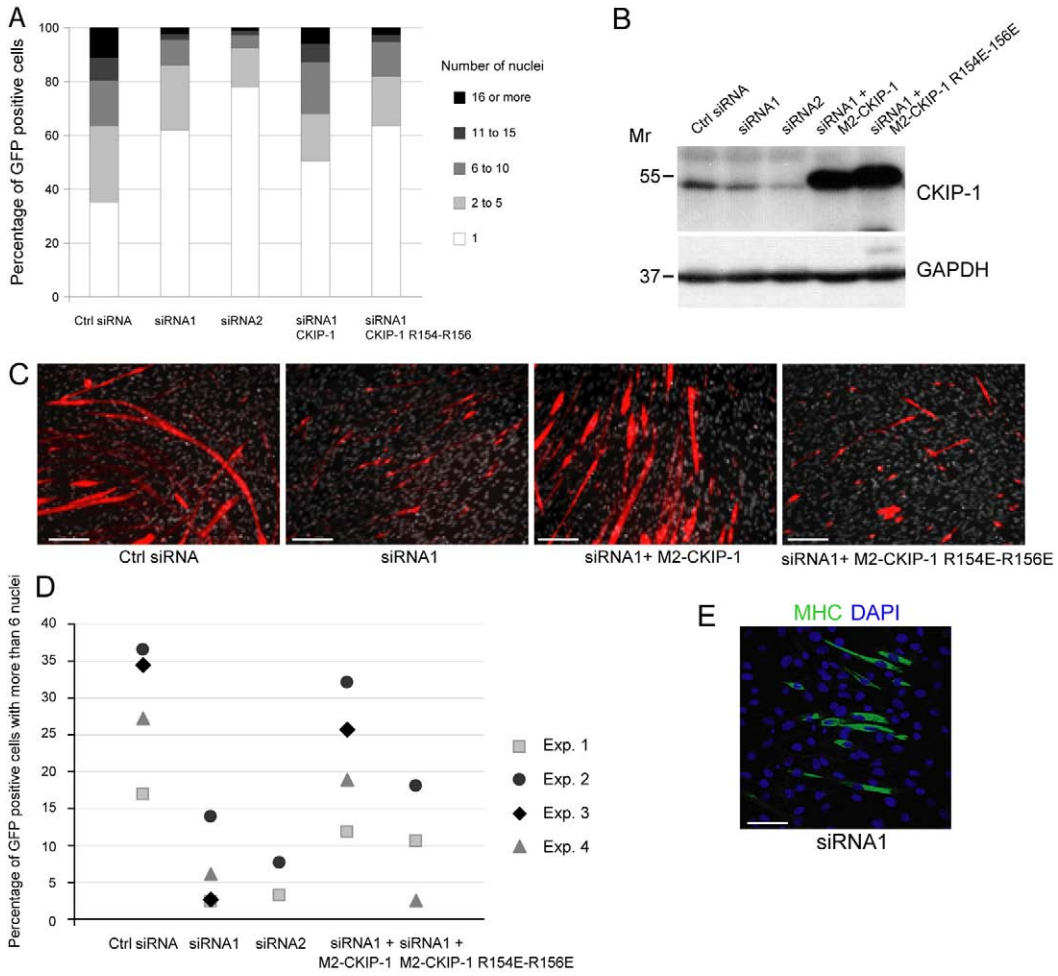

Fig. 1. siRNA-mediated inhibition of CKIP-1 blocks C2C12 myoblast fusion. (**A**) C2C12 cells were transfected with control siRNA, siRNA1, siRNA2 and empty pcDNA3 vector, siRNA1 wild-type CKIP-1 or mutant CKIP-1 R154E-R156E vectors. A GFP-expressing plasmid was included in all transfections. Cells were allowed to differentiate in differentiation medium for 4 days and were stained with DAPI to visualize nuclei. Transfected cells, identified by green fluorescence were observed by microscopy. The number of nuclei in more than 250 GFP-positive cells were counted. One representative experiment is shown. Ectopic expression of wild-type CKIP-1 restored the fusion impaired by CKIP-1 knock down with both siRNAs. (**B**) Knock down of CKIP-1 in C2C12 cells monitored by western blotting. GAPDH was used as loading control. (**C**) Representative images of cells transfected with control siRNA, siRNA1 alone or with wild-type CKIP-1 or mutant CKIP-1 R154E-R156E after 4 days of differentiation. GFP and DAPI were changed to red and grey, respectively, to allow a better visualization. Scale bars: 150 μm. (**D**) The percentage of the total counted cells with more than six nuclei in four independent experiments. (**E**) Cells were transfected with siRNA1, allowed to differentiate for 4 days and stained with DAPI (blue) and anti-MHC (myosin heavy chain; green) to visualize nuclei and differentiating myoblasts/myotubes, respectively. Scale bar: 75 μm. CKIP-1 knock down does not affect the genetic programme of differentiation.

The spatial distribution of *ckip1* expression during zebrafish development was analysed by in situ hybridization (ISH) on whole embryos at different stages (supplementary material Fig. S2). Whole mount ISH with a digoxigenin-labelled *ckip-1* antisense probe complementary to the PH domain showed a strong and diffuse expression of *ckip-1* mRNA throughout the embryo as early as the one-cell stage, indicating that *ckip-1* is maternally derived. The signal localised ubiquitously in the embryos until the end of somitogenesis. At 26 somite stage, *ckip-1* mRNA was detected in the head region and in the developing somites (supplementary material Fig. S2A). Similar results were obtained with an antisense probe (nt 1144–1548) complementary to the C-terminal part of Ckip-1 (data not shown). *Ckip-1* expression was further analysed by western blot using an anti CKIP-1 antibody, previously characterized in (Safi et al., 2004) that recognizes zebrafish Ckip-1 protein (supplementary material Fig. S2B). It shows that Ckip-1 is expressed at significant levels from one cell stage to 22 hpf (hours post fertilization) (26 somites) and is downregulated afterwards.

Ckip-1 knock down impairs fast-twitch muscle precursor fusion

Since in vitro experiments revealed that CKIP-1 is necessary for myoblast fusion, we investigated for its requirement in myoblast fusion in vivo in zebrafish. In fast muscle lineage, Ckip-1 localised at the periphery of fast precursor cells, closed to the plasma membrane visualized by beta catenin staining (Fig. 2A). To investigate a possible requirement of Ckip-1 in myoblast elongation and fusion, its expression was knocked down using two different antisense morpholino oligonucleotides (MO1 and MO2) directed against the 5′ UTR of *ckip-1* mRNA. Knock down efficiency of each morpholino antisense oligonucleotides was

assessed by immunofluorescence (supplementary material Fig. S3A) and western-blot analysis (supplementary material Fig. S3B). To help with delineation of individual cells for fusion and cell shape analysis, we mosaically labelled cell membranes in CKIP-1 morphants or control embryos, by injecting membrane-mCherry mRNA (Megason, 2009) in the cell mass at the 16–32 cell stage. The injected embryos were fixed at 24–26 hpf, stained for Prox 1 that allows slow fibre nuclei visualisation, and analysed by confocal microscopy. Fast–twitch muscle cell elongation and fusion (Cortés et al., 2003; Henry and Amacher, 2004) proceed not only in a medial to lateral wave but also in an anterior to posterior direction; thus, in any given embryo, somite differentiation is more advanced in anterior than posterior somites, and in any given somite, medial fast fibres are more mature than lateral ones. We first quantified the medial to lateral progression by counting the number of multinucleated muscle cell between the notochord and the slow fibres at the level of somite XII (mid-trunk). The majority of membrane-mCherry-positive myoblasts in CKIP-1 MO embryos was not elongated and did not span the somite width at the surface as well as throughout the mediolateral axis of the myotome (Fig. 2B). A substantial proportion (95%) of them was mononucleated (Fig. 2C). At the same level (somite XII), control embryos formed syncytial fast fibres (Fig. 2B) and 91% of mCherry-positive fibres were multinucleated (Fig. 2C). The number of nuclei per fibre in the rare fused Ckip-1 MO fibres (2.311±0.395) was not significantly different from that observed in control embryos (2.67±0.336; data not shown). As expected, in recently formed posterior somites (somite XVIII) of control MO embryos, only 34±19.4% of cells had fused, showing the anterior to posterior progression of fast-twitch muscle cell formation (Fig. 2C). Impaired fusion in CKIP-1 MO embryos is not due to a delayed anterior to posterior differentiation progression and thus a developmental delay since the same percentage of non fused cells was observed more anteriorly in somites IV as in somites XII (Fig. 2B,C).

Examination of embryos at 18 hpf showed that in contrast to what is observed in wild-type embryos, the morphology of Ckip-1 MO embryo fast precursors remained irregular and most of them did not extend protrusions in the direction of elongation and between other cells (Fig. 2D). Indeed, in wild-type embryos, short fast muscle precursor cells elongate and intercalate along the anteroposterior axis.

In Ckip-1 MO embryos, expression of the muscle determination gene, *myoD*, was unaffected; indicating that the fast-muscle precursor fusion defect was unlikely to have arisen from a general impairment in their commitment to myogenesis (supplementary material Fig. S4). Moreover, similarly to what observed in wild-type embryos, the unfused myoblasts of Ckip-1 MO embryos were also stained by monoclonal antibody F310, which specifically recognizes zebrafish fast myosin heavy chain (Fig. 2E) suggesting that mononucleated fast myoblasts were nevertheless capable of differentiating as mononucleated muscles of the fast-twitch type. Altogether, these results show that CKIP-

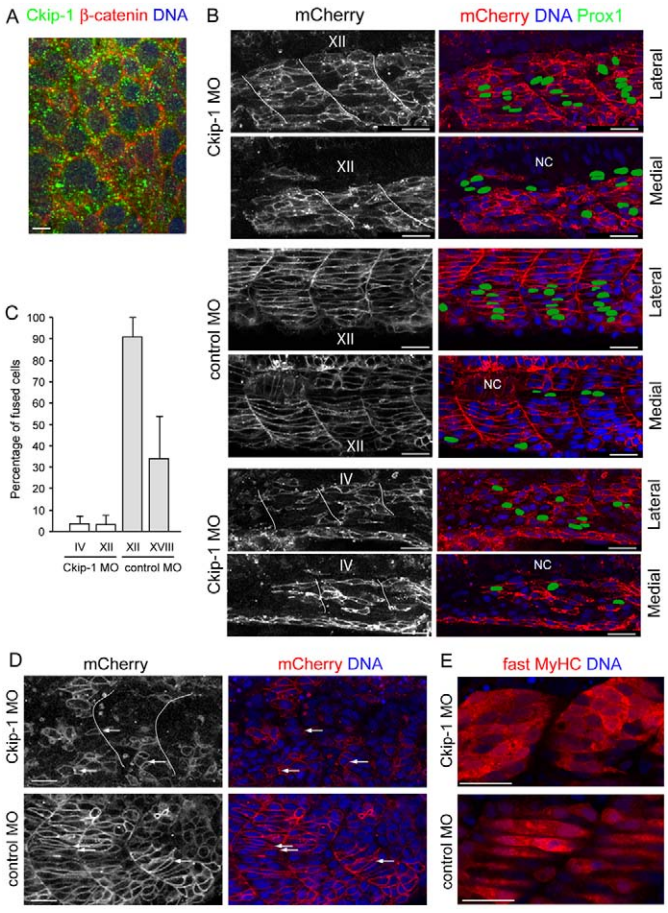

Fig. 2. Ckip-1 knock down impairs fast-twitch muscle precursor fusion. (**A**) Confocal image of Ckip-1 distribution in fast-twitch precursor cells, in an 8- to 10-somite embryo. Membranes were labelled using beta-catenin staining and nuclei with DAPI. Ckip-1 accumulates at the periphery of fast precursor cells. Dorsal view, anterior to the top. Scale bar: 5 μm. (**B**) All panels (side view, anterior to the left) are confocal images showing myocytes in three somites, in 24 hpf embryos injected at the 1-cell stage with ckip-1 or control morpholinos and subsequently reinjected with membrane-mCherry mRNA at the 16- to 32-cell stage for membrane scatter labelling. Embryos were labelled with anti-Prox1 that stains slow fibre nuclei (green) and DAPI (blue). Prox1-positive nuclei were delineated and coloured green to be more visible. The Roman numerals above a somite indicate its positioning along the anterior–posterior axis (with I designating the anterior-most somite). Two images are shown for each embryo, one at the periphery of the myotome (lateral) and one at the level of the notochord (NC; medial). In morphant embryos, myosepta are delineated in white. Scale bars: 25 μm. The membrane-mCherry staining was used to outline cells in confocal z-stacks (10–15 focal planes scanning the entire myotome), in order to count their nuclei. (**C**) Quantification of B, presented as the percentage of fused cells, i.e. containing more than one nucleus. Roman numerals under the bars indicate the analysed somite region. Values are means ± s.e.m. of six different morphant and control embryos. An average of 500 mCherry-positive cells was counted for each embryo. Whereas slow muscle fibres have reached the lateral myotome in the analysed regions (B), the fusion percentage is very low in *ckip-1* morphants compared to controls, including in more anterior (more differentiated) somites (C). (**D**) Confocal images (mid-trunk, anterior to the left) encompassing a two-somite width view of 18 hpf embryos injected with Ckip-1-MO or control MO and mCherry mRNA, labelled with DAPI (blue). Arrows show short and elongating cells in 18 hpf Ckip-1 MO- and control-MO-injected embryos, respectively. Whereas in wild-type embryos, short fast muscle precursor cells elongate and intercalate along the anteroposterior axis, they remained irregular and most of them did not extend protrusions in the direction of elongation and between other cells. Scale bars: 25 μm. (**E**) Confocal images showing a lateral view of two somites in 18 hpf Ckip-1-MO- and control-MO-injected embryos labelled for fast MyHC (F310; red) and DAPI (blue). Mid-trunk, anterior to the left. Scale bars: 25 μm. Ckip-1 knock down does not interfere with differentiation.

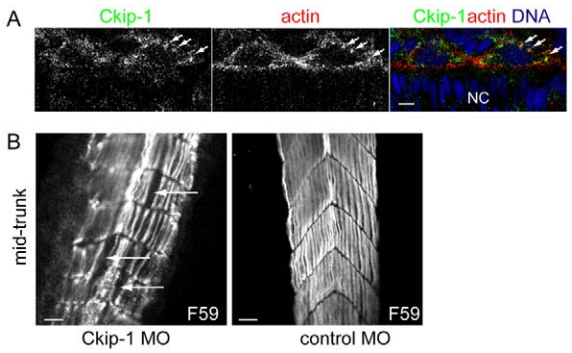

Fig. 3. Ckip-1 knock down does not affect slow muscle cell migration through the fast myotome. (**A**) Confocal image of adaxial cells at the depth of the notochord in 8- to10-somite embryos (14 hpf) labelled with Ckip-1 (green), phalloidin (red) and DAPI (blue). Dorsal view. Arrows indicate Ckip-1 colocalisation with actin. NC: notochord. Scale bar: 5 µm. (**B**) Single frames of a 3D reconstitution encompassing a five-somite width lateral view of 48 hpf Ckip-1-MO- and control-MO-injected embryos labelled with F59 antibody (grey) that stains slow fibres. Anterior to the top. Arrows indicate gaps in the lateral palisade of slow muscle fibres. Scale bars: 25 µm.

1 knock down impairs fast myoblast elongation and fusion without interfering with the differentiation genetic program.

Lack of fusion is not due to slow fibre migration defect through the fast myotome

As slow muscle fibres migrate through the somite, they act as organizers to instruct a morphogenetic wave of fast muscle cell elongation leading to fusion (Snow et al., 2008). The Hedgehog (Hh) signalling that originates from the notochord and the neural tube specifies slow myoblasts and regulates slow muscle fibre type development in zebrafish (Hirsinger et al., 2004; Lewis et al., 1999; Blagden et al., 1997). In *ckip-1* MO embryos, we observed no defects in notochord *shh* expression and in adaxial cell expression of two Hh targets, the patched 1 (*ptc1*) Hh receptor and *myoD* (supplementary material Fig. S4A,B). This suggests that the Hh pathway is intact and functional. The slow muscle-specific homeobox gene *prox1* (supplementary material Fig. S4C) was also expressed in these embryos, indicating that slow muscle fibres were specified in *ckip-1* morphants.

We observed that Ckip-1 is expressed in slow muscle precursors. Whole mount immunofluorescence followed by confocal microscopy in 8 to 10 somite embryos detected Ckip-1 accumulations, colocalised with actin cytoskeleton in .adaxial cells elongating anteroposteriorly along the notochord (Fig. 3A). In these cells, Ckip-1 was enriched at the actin-rich attachment sites to somite boundaries and colocalised with actin fibres (Fig. 3A). We investigated if *ckip-1* knock down in slow muscle precursors affects their migration. As seen in Fig. 2B, slow fibres expressing Prox 1 were seen laterally in both morphant and control animals showing that they had reached the myotome periphery. To investigate slow fibre morphology and differentiation, we stained 24 hr post fertilization (hpf) embryo cryosections with F59 antibody for slow myosin heavy chain. Confocal analysis revealed that slow fibre maturation in Ckip-1 MO embryos appeared unaltered (Fig. 3B). However, somites were more U-shaped than organized in the characteristic chevron pattern. Occasional gaps in the lateral palisade of slow muscle fibres were observed (Fig. 3B). However, those gaps are unlikely the cause of fast-twich myoblast fusion defect. Indeed, it was shown that in a Hh pathway mutant displaying neither slow muscle migration nor fast muscle cell fusion, transplantation of a single wild-type slow muscle fibre can rescue elongation of many fast muscle cells within the somite in which it is migrating (Henry and Amacher, 2004). These results show that Ckip-1 knock down did not prevent slow fibre specification, formation, migration and differentiation, strongly suggesting that fast twitch myoblast fusion defect do not arise from an aberrant slow fibre development.

CKIP-1 interacts with Arp2/3 subunit ARPC1A

To elucidate the mechanism of action of CKIP-1 in cell fusion, a yeast two hybrids screen was performed to identify new CKIP-1 interactors (Pilot-Storck et al., 2010). The Arp2/3 subunit ARPC1A was identified as a direct binding partner for CKIP-1 (Fig. 4A). This interaction was confirmed by coimmunoprecipitation of CKIP-1 and ARPC1A in cell lysates of insulin stimulated C2C12 cells (Fig. 4B). The ARPC2 subunit was also detected in CKIP-1 immunoprecipitates, indicating that ARPC1A/CKIP-1 interaction preserved the functional role of ARPC1A in assembling ARP proteins. Consistently, a colocalisation of ARPC1A and ARPC2 with CKIP-1 was observed in cell protrusions (Fig. 4C).

To identify CKIP-1 domains involved in Arp2/3 binding, we generated CKIP-1 deletion mutants (Fig. 4D). Preliminary observations showed that CKIP-1 mutants that did not interact with CP also lost their ability to immunoprecipitate Arp2/3 (data not shown). We thus generated deletion mutants encompassing CP binding domains identified in CKIP-1 (Canton et al., 2006) and other CP binding proteins (Hernandez-Valladares et al., 2010; Takeda et al., 2010) and tested their ability to co-immunoprecipitate with Arp2/3 and CP. Two main regions (residues 138–144 and residues 150–166 in human CKIP-1) were shown to be involved in CP binding and inhibition. In particular, mutation of residues Arg155 and Arg157 located in the second region fully abrogates human CKIP-1 interaction with CP (Canton et al., 2006). Deletion of the first 131 or 136 residues encompassing the PH domain (residues 20–131) did not impair Arp2/3 and CP binding to CKIP-1 (Fig. 4E). Deleting the next 10 residues (137–146) that constitute the first region (residues 137–143 in mouse CKIP-1) (Hernandez-Valladares et al., 2010) described as essential for CP alpha binding drastically reduced Arp2/3 binding. As expected, no variation in CP beta binding was observed but contrary to what was described by Hernandez-Valladares and colleagues, CP alpha binding to CKIP-1 was not altered (Hernandez-Valladares et al., 2010). Successive deletions in the second CP binding domain (residues 149–165 in mouse CKIP-1) were then tested. CP beta binding was greatly reduced when residues 147–151 were deleted. The absence of CP alpha staining is most probably due to a difference in affinity between the antibodies used for CP alpha and beta detection since no evidence for dissociation of these two subunits of the CP heterodimer have been shown in the literature. Further deletion of residues 152–156 abolished CP alpha and beta binding. In agreement with Canton et al. studies, mutation of residues 154 and 156 completely abolished CP alpha and beta binding. These mutations also ablated Arp2/3 binding (Canton et al., 2006).

Altogether, these results first show that CKIP-1 binding domains to Arp2/3 and CP are tightly linked. Residues 137–156, identified through their ability to inhibit CP and to uncap CP-bound actin filaments in other studies, are also involved in

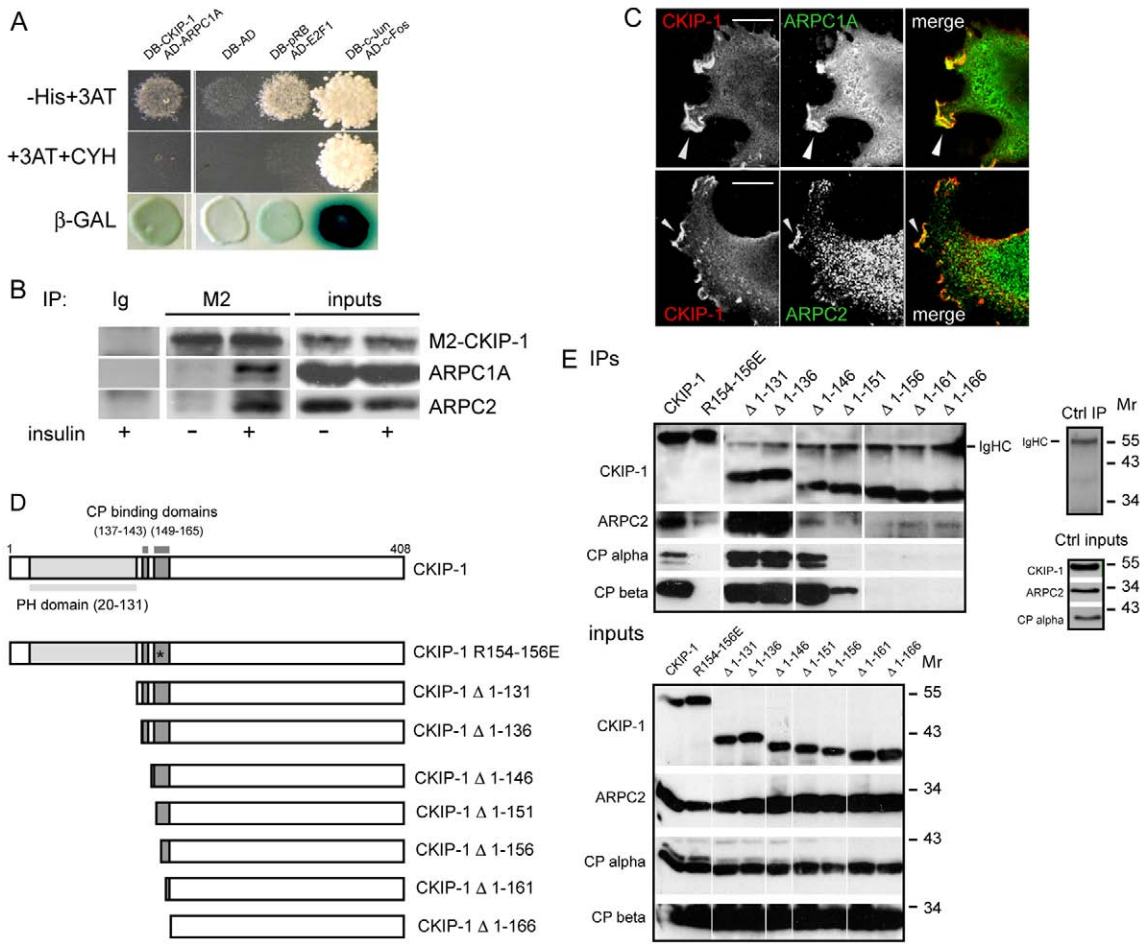

Fig. 4. CKIP-1 interacts with the Arp2/3 subunit ARPC1A and colocalises with ARPC1A and ARPC2 in membrane protrusions. (**A**) Yeast two-hybrid assay of ARPC1A and CKIP-1 protein interaction. The following controls were spotted: negative control, empty DB and AD vectors; positive controls, DB-pRB with AD-E2F1 and DB-c-Jun with AD-c-Fos. DB: DNA-binding domain, AD: activation domain. Yeasts were plated onto: (1) –His+3AT plates to test the expression of the *HIS3* reporter gene; (2) plates containing cycloheximide (+3AT+CYH) to detect auto-activators; and (3) YPD to determine *GAL1::lacZ* transcriptional activity by using a β-galactosidase filter assay (β-GAL). (**B**) Total lysates were prepared from M2-CKIP-1-transfected C2C12 cells serum starved for 4 hours and then stimulated (+) or not (−) with 25 μg/ml insulin for 10 min. CKIP-1 was immunoprecipitated with anti-M2-tag antibody. Mouse Ig (Ig) was used as a control. Immunoprecipitates (left panel) as well as input lysates (right panel) were immunoblotted for CKIP-1, ARPC1A and ARPC2. (**C**) Confocal images of M2-CKIP-1-transfected C2C12 cells co-stained for CKIP-1 and endogenous ARPC1A and ARPC2. Arrowheads indicate ARPC1A and ARPC2 colocalisations with CKIP-1 in membrane protrusions. Scale bars: 20 μm. (**D**) Schematic representations of the different CKIP-1 mutant proteins. (**E**) Total lysates were prepared from wild-type and mutant CKIP-1-transfected C2C12 cells after serum starvation and insulin stimulation. CKIP-1 wild-type and mutant proteins were immunoprecipitated with anti-M2 antibody. Immunoprecipitates as well as input lysates were immunoblotted for CKIP-1, ARPC2 and capping proteins CP alpha and beta. A non-transfected cell lysate was used as a control for the immunoprecipitation with the anti-M2 antibody. IgHC, immunoglobulin heavy chain. The absence of both ARPC2 and capping proteins binding to Δ1–156 and R154E–R156E CKIP-1 mutants demonstrate that CKIP-1 binding domains to Arp2/3 and CP are tightly linked.

Arp2/3 binding. Moreover, residues 154 and 156 seem to be also crucial residues for Arp2/3 binding to CKIP-1.

CKIP-1 controls actin cytoskeleton through its interaction with ARPC1A and its membrane localisation

Arp2/3 and capping protein are known to cooperate in dynamic dendritic actin networks formation under the plasma membrane leading to cellular protrusions extension (Akin and Mullins, 2008; Carlier and Pantaloni, 1997). To study the effects of CKIP-1 on cell morphology and lamellipodia formation, we performed experiments in vitro in C2C12 myoblasts. Endogenous CKIP-1 was mainly found in plasma membrane protrusions in association with F-actin network (Fig. 5A). Consistently, a marked enrichment of CKIP-1 could be observed in these structures as compared to adjacent areas at the cell periphery. In migrating C2C12 cells, CKIP-1 accumulated at the leading edges along the actin cortex (Fig. 5B). No staining was observed at the periphery of cells when anti-CKIP-1 antibody was absent showing that accumulation of CKIP-1 in membrane ruffles is specific (Fig. 5B). To determine if CKIP-1 had a functional role in actin regulation, the effects of CKIP-1 overexpression and depletion were examined in insulin stimulated C2C12 cells. In muscle cells, insulin induces actin polymerization and lamellipodia formation in a PI3K-Rac1-dependent manner (Ishikura et al., 2008) and CKIP-1 accumulates in plasma membrane protrusions induced by insulin (Safi et al., 2004). Cells overexpressing M2-tagged CKIP-1

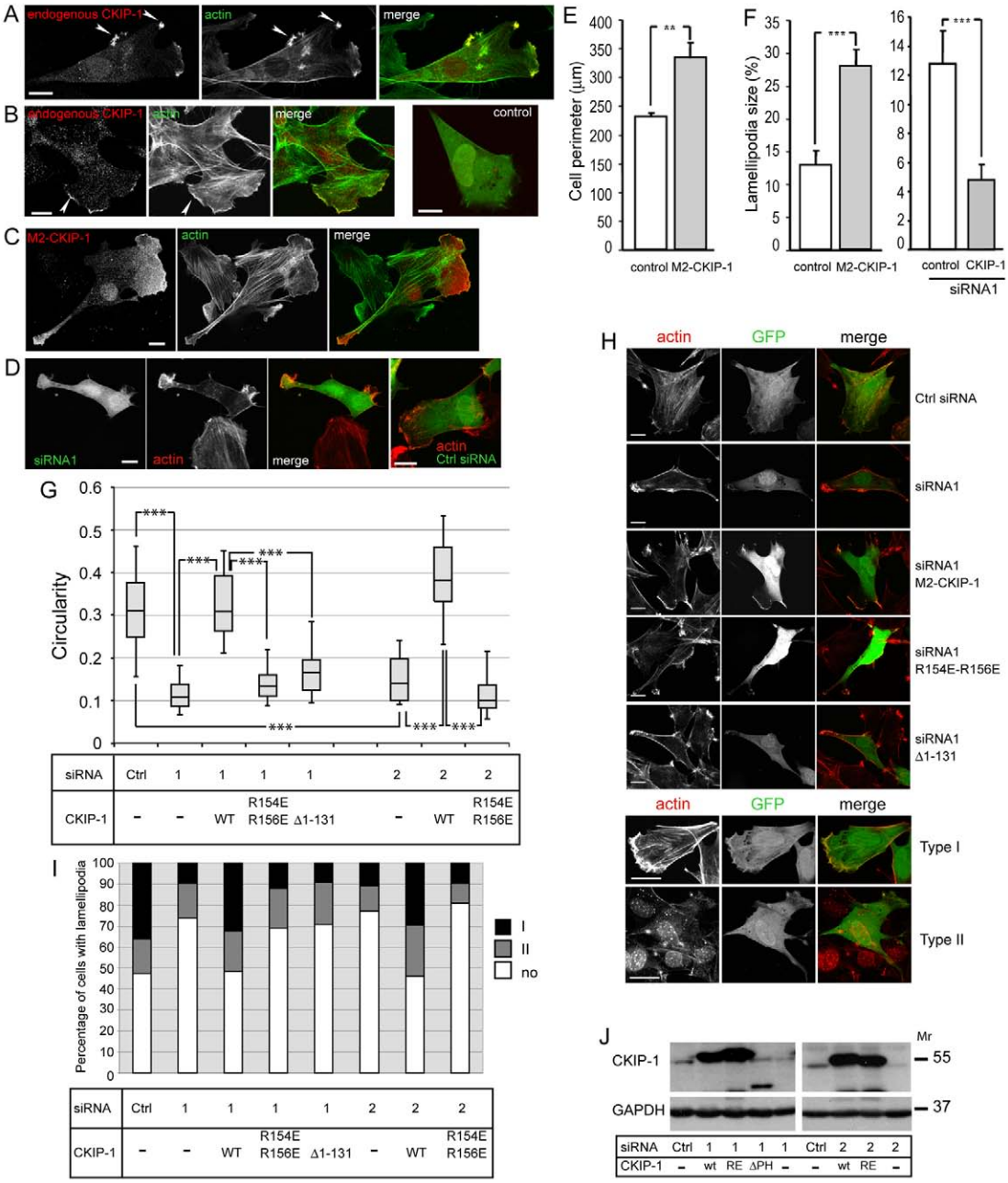

Fig. 5. Cell morphology regulation by CKIP-1 requires its binding to Arp2/3 as well as its membrane localisation. (**A**,**B**) Confocal images of C2C12 cells labelled with phalloidin and anti-CKIP-1 antibody. Arrowheads point to endogenous CKIP-1 cell surface accumulation at actin remodelling sites in cellular protrusions (A) and lamellipodia of migrating cells (B). Scale bars: 20 μm. (**C**,**D**) C2C12 cells were transfected with either M2-CKIP-1, siRNA1, control siRNA or a GFP-expressing vector were serum starved for 6 hours and then stimulated with insulin for 10 min. Cells were labelled with phalloidin and anti-CKIP-1 antibody. Scale bars: 20 μm. (**E**) The perimeter of insulin-stimulated C2C12 cells transfected with M2-CKIP-1 or control empty vector was measured using ImageJ software from confocal images taken at a z-position where the cell perimeter was maximal. Results shown are the average perimeter of ~120 cells in six different experiments; error bars indicate s.e.m. (**F**) Lamellipodia size calculated as the ratio of the membrane length constituting the lamellipodia (measurement based on actin organization) to the cell total perimeter in M2-CKIP-1- and control-transfected C2C12 cells (left graph), and control siRNA- and siRNA1-transfected cells C2C12 cells (right graphs). In E and F, statistical significance was evaluated in independent samples *t*-tests; $^{**}P<0.005$, $^{***}P<0.001$, respectively. CKIP-1 increases lamellipodia size, and inhibition of its expression suppresses their formation. (**G**) C2C12 cells were transfected with control siRNA, siRNA1, siRNA2 and empty pcDNA3, wild-type CKIP-1, mutant CKIP-1 R154E–R156E and CKIP-1 Δ1–131 vectors together with a GFP-expressing plasmid. Fifty to sixty transfected cells, identified by green fluorescence, were observed by microscopy. Circularity was measured with ImageJ software. A value of 1.0 indicates a perfect circle. As the value approaches 0.0, it indicates an increasingly elongated shape. One representative experiment out of two is shown. The box-and-whiskers plots show values of first decile (lower whiskers), first quartile (box lower limit), median, third quartile (box upper limit) and ninth decile (upper whiskers). Statistical significance was evaluated using Mann–Whitney–Wilcoxon tests; $^{***}P<0.001$. Wild-type CKIP-1 but not mutant CKIP-1 R154E–R156E and CKIP-1 Δ1–131 restored a circularity degree similar to that observed in control siRNA cells. One representative experiment is shown. (**H**) Representative images of cells analysed in G. (**I**) The presence of lamellipodia as well as their size (illustrated on the right) was analysed in the same cells used in G and H. (**J**) CKIP-1 immunoblot of extracts of C2C12 cells used in the experiments in G, H and I. GAPDH was used as a loading control. RE, mutant CKIP-1 R154E–R156E; ΔPH, CKIP-1 Δ1–131. The formation of lamellipodia was restored in cells expressing ectopic wild-type CKIP-1 but not mutant R154E–R156E and Δ1–131.

displayed larger lamellipodia (Fig. 5C). Measurements showed a 40% increase of cell perimeter in M2-CKIP-1-transfected versus control cells (Fig. 5E). More importantly, the proportion of cell perimeter involved in lamellipodia increased more than twofold in M2-CKIP-1 cells as compared to control cells (Fig. 5F, left graph). CKIP-1 knock down by siRNA (Fig. 5D) had opposite effects. C2C12 cells transfected with CKIP-1 siRNA1 or 2 and a GFP expressing vector had an elongated shape and did not extend large lamellipodia even after insulin treatment (Fig. 5D,F, right graph). These effects were not observed with a control siRNA (Fig. 5D). The circularity of siRNA 1- and 2-treated cells could be restored by transfection of wild-type CKIP-1 (Fig. 5G,H). As seen in Fig. 5H, siRNA1 transfected cell expressing M2-CKIP-1 had a more compact shape as a result of spreading and display lamellipodia. Expression of mutated CKIP-1 Δ1–131 that does bind ARPC1A (Fig. 4E) but not plasma membrane since depleted of its PH domain (Safi et al., 2004) or CKIP-1 R154E–R156E that does not bind to Arp2/3 complex anymore but still bears its PH domain and thus binds plasma membrane (Canton et al., 2006; our unpublished data) did not restored circularity and large lamellipodia formation (Fig. 5G,H). The presence of lamellipodia in siRNA and rescued cells was measured and compared to scrambled siRNA-transfected cells. We defined two types of lamellipodia; large circular lamellipodia originating from the cell body (type I) and smaller lamellipodia located at the end of cellular protrusions (type II) (Fig. 5I, pictures on the right). Forty cells were analysed. As expected (graph on the left in Fig. 5I), CKIP-1 knock down impairs lamellipodia formation. Indeed, more than 70% of cells did not form any as compared to 47% of control cells. Expression of wild-type CKIP-1, but neither Δ1–131 nor R154E–156E CKIP-1 mutants, restored the formation of lamellipodia in siRNA1- and siRNA2-transfected cells with similar percentage of type I and II lamellipodia observed in control siRNA-transfected cells. This showed that CKIP-1 abilities to bind to plasma membrane and to interact with Arp2/3 are required for cell shape regulation. Importantly, the R154E–156E CKIP-1 mutant also failed to restore C2C12 myoblast fusion (Fig. 1A–D).

Altogether, these experiments showed that CKIP-1 predominantly colocalises with cortical actin at regions of active cytoskeleton remodelling. They demonstrate that CKIP-1 regulates cellular shape and is required for cellular protrusion extension (lamellipodia) formation after insulin stimulation. Since lamellipodia are required for cell movements, decreasing CKIP-1 expression should impair cell motility. As expected (supplementary material Fig. S5), inhibition of lamellipodia formation induced by CKIP-1 depletion affects cell migration. Altogether, these results indicate that the effects of CKIP-1 on cell shape and muscle cell fusion are likely due to its ability to regulate actin cytoskeleton through the targeting of Arp2/3 at the plasma membrane.

Discussion

Membrane and cytoskeletal remodelling govern fusion and myofibre formation. Numerous studies have shown that a number of *Drosophila melanogaster* and mouse gene products linked to Arp2/3-complex-dependent actin-cytoskeleton remodelling are crucial for myoblast fusion (Rochlin et al., 2009). In zebrafish, two main studies have implicated cytoskeleton regulators; the GTPase Rac1 and its activators Dock1 and 5, in fast-twitch myoblasts fusion (Srinivas et al., 2007; Moore et al., 2007). This work strongly suggests that Arp2/3 via its interaction with CKIP-1 is also involved in zebrafish fast myoblast fusion.

Here, we show that CKIP-1 is involved in myoblast fusion in mammalian cells in vitro and in vivo in zebrafish muscle. CKIP-1 knock down resulted in a severe reduction of C2C12 myoblast fusion and of myotube formation. Similarly, inhibition of *ckip-1* expression in zebrafish abolished fast twitch myoblast fusion and thus fast fibre formation. Membrane remodelling (cell shape modifications, absence of lamellipodia formation) in CKIP-1 knockdown myoblasts in vitro is affected, suggesting that CKIP-1 regulation of membrane remodelling is a crucial event in the fusion process. Search for CKIP-1-interacting proteins identified Arp2/3 subunit ARPC1A. We show that CKIP-1 regulates cell morphology and cellular protrusion formation through cortical actin remodelling by recruiting at the plasma membrane the actin nucleator Arp2/3 complex.

CKIP-1 knock down affects morphological changes required for myoblasts fusion

Using live imaging to examine differentiating C2C12 myoblasts for evidence of actin-based behaviours during differentiation and fusion, Nowak et al. observed different myoblast behaviour during differentiation (Nowak et al., 2009). At 24 hours after switching to differentiation medium, the fibroblast-like C2C12 cells all displayed membrane ruffling and formation of lamellipodia and filopodia. At 48 hours of culture, myoblasts elongated and extended and retracted filopodia-like membrane protrusions from each tip of the long axis of the myoblast. CKIP-1 knock down in C2C12 cells abolished cell protrusion (such as lamellipodia) formation. After 72 hours in differentiation medium, 60% and 30% of control siRNA-transfected and CKIP-1 siRNA-transfected cells, respectively, did display the elongated shape (data not shown) required for fusion as described by Nowak and colleagues (Nowak et al., 2009). These morphological defects were associated with fusion defects since more than 70% of CKIP-1 knockdown cells remained mononucleated. However, CKIP-1 knockdown cells did express sarcomeric myosin heavy chain indicating that these myoblasts were capable of forming functional myotubes, provided that they were able to fuse into multinucleated structures. Thus, the absence of CKIP-1 most probably abolishes cell fusion by preventing all required morphological changes.

Investigation of the role of Ckip-1 in zebrafish myogenesis revealed that fast twitch myoblast precursor cell morphological changes were also affected in Ckip-1 knockdown embryos. In zebrafish fast muscle fibre morphogenesis consists of three phases. In the first phase, cells exhibit randomly directed protrusive activity. The second phase, intercalation/elongation, proceeds via a two-step process: protrusion extension and filling. When both the anterior and posterior ends of the muscle cell reach the myosept, they adopt the cylindrical shape of myotubes (Snow et al., 2008). In Ckip-1-deficient embryos, most myoblasts did not elongate and intercalate and remained mononucleated. However, they retained the capacity to differentiate and expressed fast MyHC. Thus, as in mammalian cells, Ckip-1 interferes with morphogenetic behaviours and fusion but not with the differentiation genetic programme. We showed that in vivo slow fibre migration is not affected in Ckip-1 MO zebrafish embryos (Fig. 3B), whereas Ckip-1 knock down in vitro in C2C12 myoblasts impedes migration (supplementary material Fig. S5). This apparent discrepancy between in vivo and in vitro

data could be explained by differences in migration 'modalities'. Slow-twitch muscle migration through the entire myotome is influenced by differential cell adhesion. Dynamic and reciprocal waves of N-cadherin and M-cadherin expression within the myotome, which correlate precisely with cell migration, generate differential adhesive environments that drive slow-twitch muscle cell migration through the myotome (Cortés et al., 2003). On the contrary, C2C12 myoblasts migrate in a 2D environment where most cells are able to move freely on dish surface by extending large membrane protrusions. Another possibility is Ckip-1 incomplete abrogation of function. Indeed, the two morpholinos we used failed to fully inhibit Ckip-1 expression, a part of which appeared to be maternally supplied. Given the ubiquitous expression and probable multiple roles of CKIP-1 in a variety of cellular processes (Lu et al., 2008; Tokuda et al., 2007; Zhang et al., 2007; Zhang et al., 2006; Zhang et al., 2005), one would expect its complete inactivation to result in much-earlier developmental arrest.

CKIP-1 regulates actin dynamics through its binding to Arp2/3 and membrane phosphoinositides

To investigate how CKIP-1 is involved in membrane remodelling that occurs during cellular protrusion extension, we performed a yeast two hybrid screen and identified ARPC1A, a subunit of Arp2/3 complex as a CKIP-1 interacting protein (Pilot-Storck et al., 2010). The ARPC2 subunit was also detected in CKIP-1 immunoprecipitates, indicating that ARPC1A/CKIP-1 interaction preserved the functional role of ARPC1A in assembling ARP proteins. ARPC1A subunit of Arp2/3 complex is important for the proper structural organization of the nucleation site and for binding to Arp2/3 activators (Gournier et al., 2001; Pan et al., 2004; Balcer, et al., 2010; Robinson et al., 2001; Zalevsky et al., 2001). CKIP-1 knock down by siRNAs led to cell morphology alterations, showing that CKIP-1 regulates actin dynamics and thus membrane remodelling. These alterations could be rescued by wild-type CKIP-1 but not by mutant CKIP-1 R154E–R156E which still binds plasma membrane (Canton et al., 2006) through its PH domain but does not bind to Arp2/3 or by mutant CKIP-1 Δ1–131 that binds Arp2/3 but is not localised at the plasma membrane (Safi et al., 2004). Thus, both membrane localisation and Arp2/3 binding are required for CKIP-1 actin dynamics regulation.

CKIP-1 interacts with actin capping protein at the barbed ends of actin filaments (Canton et al., 2005; Canton et al., 2006). Capping protein and Arp2/3 complex are known to cooperate in dynamic actin remodelling events (Akin and Mullins, 2008; Carlier and Pantaloni, 1997). When trying to delineate the interaction domains between CKIP-1 and Arp2/3 complex, we found that CKIP-1 binding domains to Arp2/3 and CP are tightly associated. Whether the requirement for CKIP-1 in myoblast fusion that we have uncovered involves its interaction with both Arp2/3 and CP remains to be determined. To our knowledge, no report on the role of CP in myoblast membrane fusion that is dependent on actin remodelling has been made and this needs to be investigated.

CKIP-1 C-termini does not resemble that of all shown NPFs, which are characterized by Arp2/3-binding CA-modules linked N-terminally to different numbers of actin monomer-binding WH2 domains (W), thus CKIP-1 is not likely to be an NPF. One hypothesis is that CKIP-1 is an adaptor such as FAM21 (Derivery et al., 2009; Gomez and Billadeau, 2009; Jia et al., 2010). Similarly to CKIP-1, FAM21 interacts directly with CAPZ and inhibits its actin-capping activity. It has been shown that FAM21 by participating to protein complexes links CP to Arp2/3 and Arp2/3 activators (such as WASH and WAVE NPFs) (Jia et al., 2010). Through its association with an NPF, CKIP-1 may recruit Arp2/3 close to the ends of actin filaments, promoting actin branching at the leading edges. We previously showed that CKIP-1 targeting at the plasma membrane depends on PI3K signalling activation (Safi et al., 2004). One can hypothesize that CKIP-1 targets an NPF containing complex to active regions of the plasma membrane in response to external cues that activate PI3K and/or induce myoblast membrane fusion.

Materials and Methods

Zebrafish husbandry

Zebrafish maintenance and embryo collection were carried out using established protocols (Westerfield, 2001). Zebrafish embryos were staged according to Halpern et al. (Halpern et al., 1995)

Morpholino oligonucleotide injections

Morpholinos (MO) were designed with sequence complementary to *ckip1* cDNA and purchased from Gene-Tools, LCC. The sequences of the two *ckip1* morpholino antisense oligonucleotides used were: ckip1 MO1 5′-TGGCTCAATGAAACA-CCGCTTCCCG-3′ (−24 to +1 of the ATG codon) and ckip1 MO2 5′-CTCTCTCCCTCCACGAACAATCCAG-3′ (−51 to −27 from the ATG codon). *ckip1* MO were injected at a concentration of 1–2 mM. The control morpholino oligonucleotide used for comparison was Gene-Tools Standard Control: CCTCTTACCTCAGTTACAATTTATA. To allow delineation of individual cells for fusion and cell shape analysis, we subsequently injected 20–40 pg of membrane-mCherry mRNA into 1 blastomere at 16–32 cell stage. pCS2-membrane–mCherry (Megason, 2009) was linearized using NotI, purified using a Qiagen nucleotide removal spin column, and used as template for in vitro transcription with the Ambion mMessage mMachine sp6 kit. In vitro transcribed RNA was purified using a Qiagen RNA cleanup column and quantitated on a NanoDrop spectrophotometer.

Whole-mount in situ hybridization

Whole-mount in situ hybridizations were performed according to Thisse and Thisse (http://www-igbmc.u-strasbg.fr/zf_info/zbook/chapt9/9.82.htlm). Riboprobe for *ckip1* was transcribed from a template comprising 319 bp from nt 38-357 localised within the PH domain. A sense RNA probe complementary to the specific *ckip1* probe was prepared as negative control. The *myoD* (Odenthal et al., 1996), *ptc* and *shh* RNA probes were prepared as previously described (http://www-igbmc.u-strasbg.fr/zf_info/zbook/chapt9/9.82.htlm) (Thisse et al., 2004). Embryos were observed on a LUMAR stereomicroscope (Zeiss).

Immunochemical staining

Immunofluorescence labelling on embryo frozen sections was performed as previously described (Bader et al., 2009). For whole-mount immunofluorescence labelling, embryos were fixed overnight at 4℃ in 4% paraformaldehyde. Fixed embryos were blocked and permeabilised using a solution containing 5% goat serum and 0.5% Triton X-100 in PBS. Embryos were incubated with F59 and F310 antibodies (Developmental Studies Hybridoma Bank, University of Iowa, USA), β-catenin antibody (Sigma), Phalloidin 488 and TOTO-3 iodide 642-660 (Invitrogen). After an overnight incubation with primary antibodies at 4℃, embryos were extensively washed in PBS at room temperature and incubated with the secondary antibody conjugated to Alexa Fluor 488 or Alexa Fluor 555 (Invitrogen) at room temperature for 1 hr. Sections and whole-mount embryos were observed using a spectral confocal laser scanning microscope (TCS SP5; Leica). Leica confocal software (LAS AF) was used for confocal acquisition. For all imaging, exposure settings were identical between compared samples. Images were processed using Adobe Photoshop software.

Cell lines, culture conditions, transfections, reagents and antibodies

C2C12 cells (ATCC number CRL-1772^{TM}) were grown at 37℃ under 5% CO_2. Cells were maintained as myoblasts in growth medium: Dulbecco's Modified Eagle Medium (DMEM, PAA) supplemented with 15% fetal calf serum (PAA). Cells were differentiated in differentiation medium: DMEM supplemented with 2% horse serum (Gibco BRL). Human recombinant insulin (Sigma) was used at 25 μM. Cell transfections with plasmids were performed with jetPRIME (Polyplus-transfection) according to the manufacturer's instructions. siRNA or siRNAs and plasmid transfections, using jetPRIME were performed as follows: 300,000 C2C12 cells were seeded in 35 mm diameter tissue culture dishes and

transfected 3 h later with 100 pmol siRNA and either empty pcDNA3 vector or wild-type and mutant-CKIP-1-expressing vector. A second identical transfection was realized 24 hours later. 48 hours after the first transfection, cells were trypsinised and seeded at 150,000 cells per 35 mm dish. 24 hours later (i.e. 72 hours after the first transfection), cells were used in the different experiments. Anti CKIP-1 antibody has been described previously (Safi et al., 2004). It was raised against a peptide encoding 15 amino acids (241–255) in the carboxy-terminal part of mouse CKIP-1. The other antibodies were: mouse monoclonal anti M2-FLAG (Sigma), rabbit anti-GAPDH (Sigma), rabbit polyclonal anti ARPC2 (Upstate Biotechnology) and ARPC1A, provided by the Welch Laboratory. Anti-CPα (MAb 5B12.3) and-CPβ (MAb 3F2.3) subunits of the actin capping protein and mouse monoclonal anti-myosin heavy chain (MAb F59, slow fibres and F310, fast fibres) were obtained from the Iowa Hybridoma Bank developed under the auspices of the National Institute of Child Health and Human Development and maintained by the Department of Biological Sciences, University of Iowa (Iowa City, Iowa). Actin filaments were stained with Phalloidin Alexa Fluor 488 or 555 (Invitrogen). Secondary antibodies for immunofluorescence were goat anti mouse and rabbit Alexa Fluor 555 and Alexa Fluor 488 (Invitrogen). Secondary antibodies used in western blot analysis were horseradish peroxidase (HRP)-conjugated sheep anti-mouse IgG and donkey anti-rabbit IgG (Amersham Biosciences).

Plasmid constructs

Full-length cDNA encoding M2-FLAG-tagged wild-type (Safi et al., 2004) and mutant CKIP-1 were subcloned into pcDNA3 vector (Invitrogen).

FLAG–CKIP-1 R154-156E [CKIP-1 mutant defective for CP interaction (Canton et al., 2006)] was generated by PCR amplification as previously described (Mal et al., 2004) using the Phusion Hot Start High-Fidelity DNA Polymerase (Finnzyme) with the following forward primer: 5′-CCTACTGAAGACGAAGCAAAAATCCAACACTCCCGCCGTCCTC-3′, and reverse primer: 5′-TTTTGCTTCGTCTTCAGTAGGGTGGGCAAGATAGCTGTCCTCCTC-3′. FLAG–CKIP-1 Δ1–131, FLAG–CKIP-1 Δ1–136, FLAG–CKIP-1 Δ1–141, FLAG–CKIP-1 Δ1–146, FLAG–CKIP-1 Δ1–151, FLAG–CKIP-1 Δ1–156, FLAG–CKIP-1 Δ1–161, and FLAG–CKIP-1 Δ1–166 were generated using M2-FLAG-tagged wild-type CKIP-1 as a template, the following forward primers: 5′-CGCGCGGAATTCAGAGCTAAAAACCGTATCTTGG-3′, 5′-CGCGCGGAATTCATCTTGGATGAGGTCACCG-3′, 5′-CGCGCGGAATTCACCGTTGAGGAGGACAG-3′, 5′-CGCGCGGAATTCAGCTATCTTGCCCACCCTA-3′, 5′-CGCGCGGAATTCCCTACTCGAGACAGAGC-3′, 5′-CGCGCGGAATTCGCAAAAATCCAACACTCCC-3′, 5′-CGCGCGGAATTCTCCCGCCGTCCTCCA-3′ and 5′-CGCGCGGAATTCACCCGGGGACACCTC-3′, respectively, and the same reverse primer: 5′-CAATCAGCGGCCGCACTAGTCT-3′. The resulting PCR fragments were subcloned into the EcoRI–NotI sites of M2-FLAG-tagged wild-type CKIP-1. CKIP-1 siRNA was previously described (Safi et al., 2004).

siRNA sequence and transfection

Stealth RNA siRNAs duplexes (Invitrogen) were designed by Invitrogen to target sequences in *Ckip-1* ORF: siRNA1, siRNA2, 5′-GAUCCAGGACCUGGUAGCAAGGAAA-3′ (nt 918–942) and 5′-CCUCAGAUGGGAUGCUAACAUUAGA-3′ (nt 536–560), respectively. A scramble siRNA not homologous to any sequence in vertebrate transcriptome, tested not to induce stress response and with a 45 to 55% GC content (Stealth RNAi siRNA Negative Control Med GC, Invitrogen) was used as a control.

Western blot analysis

Embryos and cells were lysed in buffer (100 mM Tris-HCl, pH 7.5, 2 mM EDTA, 100 mM NaCl, 1% Triton X-100, protease and phosphatase inhibitors (Complete, Roche Molecular Biochemicals). Protein concentrations were determined using the Bio-Rad DC kit (Bio-Rad). 20 µg total proteins were separated by 11% SDS-PAGE electrophoresis and transferred onto PVDF membranes (Hybond P, GE Healthcare). Membranes were blocked with TBS–0.02% Tween containing 5% skimmed milk and incubated overnight at 4℃ with primary antibodies. Membranes were washed and incubated for 30 min with anti-mouse and anti-rabbit HRP-conjugated secondary antibodies (Amersham Biosciences). After several washes in TBS–0.02% Tween, membranes were incubated with ECL$^+$ reagent (GE Healthcare).

Immunofluorescence analysis

Immunofluorescence analysis was performed as follows. Cells were fixed for 20 min in 4% paraformaldehyde–PBS prior to permeabilisation for 10 min with 0.1% Triton X-100 in PBS and saturation for 30 min with 1% BSA in PBS. Cells were then incubated with the primary antibodies diluted in PBS with 1% BSA for 2 hours at room temperature or overnight at 4℃, then washed in PBS, and incubated for 1 hour with secondary antibodies. DAPI that stains DNA was added to the secondary antibodies.

Labelled cells were observed with a spectral confocal laser scanning microscope (TCS SP5; Leica). Leica confocal software (LAS AF) was used for confocal acquisition. For all imaging, exposure settings were identical between compared samples. Images were processed using Adobe Photoshop and ImageJ (Abramoff et al., 2004) software.

Time-lapse video microscopy

Cells were maintained at 37℃, 6% CO_2 in relative humidity. They were grown on 0.10-mm thick tissue culture dish and studied for 15 hours after serum starvation and wound healing. Video time-lapse was realized with an inverted microscope Axiovert 100 M Zeiss, Germany (objective 10×, numeric aperture, 0.25). Cell images were captured in transmitted illumination (exposure time, 10 ms) every 10 min for 15 hours as time series of 16-bit files. Paths and trajectories of 25 cells per experiment during 840 min were analysed with Metamorph software. First phase contrast image of 86 sequential images (every 10 min) was pseudocoloured green, last image was pseudocoloured red and the images were superimposed.

Co-immunoprecipitation experiments

Cells were transiently transfected with pcDNA3 CKIP-1 wild-type and mutants. Cells were washed twice in cold PBS and lysed on ice in 50 mM Tris-HCl (pH 7.5), 10% glycerol, 150 mM NaCl, 1% NP40 and protease and phosphatase inhibitors (Complete, Roche Molecular Biochemicals; 2 mM β-glycerophosphate, sodium orthovanadate 1 mM and sodium fluoride 10 mM). Lysates were centrifuged for 10 min at 14,000 rpm at 4℃, and protein concentrations were measured in supernatants. Lysates were precleared by incubation for 30 min with proteins A/G Sepharose beads. After centrifugation, antibodies were added to supernatants for 4 hours at 4℃. Next, 60 µl of proteins A/G Sepharose beads were added to supernatants for 1 hour at 4℃. Beads were washed three times in lysis buffer. Total proteins and co-immunoprecipitates were analysed by western blotting.

Yeast two-hybrid experiments

CKIP-1 and ARPC1A human open reading frames were transferred by recombinational cloning into pDB-dest and pAD-dest-CYH destination vectors to generate DB-ORF and AD-ORF fusions, respectively (Rual et al., 2004). DB-ORF and AD-ORF were transformed individually into MaV203 yeast strain. DB-ORF- and AD-ORF-transformed cells were spotted on solid synthetic complete (Sc) media lacking leucine (Sc-L) or tryptophan (Sc-W), respectively. Then, they were plated on Sc-L-W plates lacking histidine and containing 20 mM 3-AT (Sc-L-W-H+3AT) to select for colonies that exhibited elevated expression levels of the GAL1::HIS3 yeast two-hybrid marker. After 5 days at 30℃, colonies were consolidated on Sc-L-W-H+3-AT plates and then transferred to Sc-L-W-H+3AT and Sc-L-W-U plates to confirm GAL1::HIS3 and SPAL10::URA3 transcriptional activity and to solid medium containing yeast extract, peptone and dextrose (YPD) to determine GAL1::lacZ transcriptional activity using a β-galactosidase filter assay. The interaction was retested by mating DB-CKIP-1 to AD-ARPC1A yeasts. After one day, the cells were transferred on Sc-L-W to select for diploids. After 1 day, the diploids were plated on to Sc-L-W-H+3AT, to YPD and to Sc-L+3AT plates containing tryptophan and cycloheximide (Sc-L+3AT+CYH). The pAD-dest-CYH vector contains the CYH2 negative selection marker that allows plasmid shuffling on cycloheximide-containing media. This step allowed us to check that no auto-activation arose (Li et al., 2004).

Acknowledgements

We are grateful to M. D. Welch (Department of Molecular and Cell Biology, University of California) for providing Arp2/3 subunit antibodies. The (MAb 5B12.3) (MAb 3F2.3), (MAb F59) (MAb F310) were obtained from the Developmental Studies Hybridoma Bank developed under the auspices of the NICHD and maintained by The University of Iowa, Department of Biology, Iowa City, IA 52242. We thank the zebrafish (PRECI) and microscopy (Plateau Technique Imagerie/Microscopie) facilities of the IFR128 Biosciences.

Funding

This work was supported by the Association française contre les Myopathies [grant number AFM-12130 to F.C. and E.G.]; the Ministère de la Recherche et de l'Enseignement Supérieur; Fondation pour la Recherche Médicale [grant number FDT20101221104 to A.G.]; the Association pour la Recherche contre le Cancer [grant number ARC-3853 to E.G.]; and the Ministère de la Recherche et de la Technologie [grant number ANR-11-BSV2-017-01 to L.S.].

Supplementary material available online at
http://jcs.biologists.org/lookup/suppl/doi:10.1242/jcs.101048/-/DC1

References

Abmayr, S. M. and Pavlath, G. K. (2012). Myoblast fusion: lessons from flies and mice. *Development* **139**, 641-656.

Abramoff, M. D., Magelhaes, P. J. and Ram, S. J. (2004). Image Processing with ImageJ. *Biophotonics International* **11**, 36-42.

Akin, O. and Mullins, R. D. (2008). Capping protein increases the rate of actin-based motility by promoting filament nucleation by the Arp2/3 complex. *Cell* **133**, 841-851.

Bader, H. L., Keene, D. R., Charvet, B., Veit, G., Driever, W., Koch, M. and Ruggiero, F. (2009). Zebrafish collagen XII is present in embryonic connective tissue sheaths (fascia) and basement membranes. *Matrix Biol.* **28**, 32-43.

Balcer, H. I., Daugherty-Clarke, K. and Goode, B. L. (2010). The p40/ARPC1 subunit of Arp2/3 complex performs multiple essential roles in WASp-regulated actin nucleation. *J. Biol. Chem.* **285**, 8481-8491.

Blagden, C. S., Currie, P. D., Ingham, P. W. and Hughes, S. M. (1997). Notochord induction of zebrafish slow muscle mediated by Sonic hedgehog. *Genes Dev.* **11**, 2163-2175.

Bosc, D. G., Graham, K. C., Saulnier, R. B., Zhang, C., Prober, D., Gietz, R. D. and Litchfield, D. W. (2000). Identification and characterization of CKIP-1, a novel pleckstrin homology domain-containing protein that interacts with protein kinase CK2. *J. Biol. Chem.* **275**, 14295-14306.

Canton, D. A., Olsten, M. E., Kim, K., Doherty-Kirby, A., Lajoie, G., Cooper, J. A. and Litchfield, D. W. (2005). The pleckstrin homology domain-containing protein CKIP-1 is involved in regulation of cell morphology and the actin cytoskeleton and interaction with actin capping protein. *Mol. Cell. Biol.* **25**, 3519-3534.

Canton, D. A., Olsten, M. E., Niederstrasser, H., Cooper, J. A. and Litchfield, D. W. (2006). The role of CKIP-1 in cell morphology depends on its interaction with actin-capping protein. *J. Biol. Chem.* **281**, 36347-36359.

Carlier, M. F. and Pantaloni, D. (1997). Control of actin dynamics in cell motility. *J. Mol. Biol.* **269**, 459-467.

Cortés, F., Daggett, D., Bryson-Richardson, R. J., Neyt, C., Maule, J., Gautier, P., Hollway, G. E., Keenan, D. and Currie, P. D. (2003). Cadherin-mediated differential cell adhesion controls slow muscle cell migration in the developing zebrafish myotome. *Dev. Cell* **5**, 865-876.

Derivery, E., Sousa, C., Gautier, J. J., Lombard, B., Loew, D. and Gautreau, A. (2009). The Arp2/3 activator WASH controls the fission of endosomes through a large multiprotein complex. *Dev. Cell* **17**, 712-723.

Devoto, S. H., Melançon, E., Eisen, J. S. and Westerfield, M. (1996). Identification of separate slow and fast muscle precursor cells in vivo, prior to somite formation. *Development* **122**, 3371-3380.

Gomez, T. S. and Billadeau, D. D. (2009). A FAM21-containing WASH complex regulates retromer-dependent sorting. *Dev. Cell* **17**, 699-711.

Gournier, H., Goley, E. D., Niederstrasser, H., Trinh, T. and Welch, M. D. (2001). Reconstitution of human Arp2/3 complex reveals critical roles of individual subunits in complex structure and activity. *Mol. Cell* **8**, 1041-1052.

Halpern, M. E., Thisse, C., Ho, R. K., Thisse, B., Riggleman, B., Trevarrow, B., Weinberg, E. S., Postlethwait, J. H. and Kimmel, C. B. (1995). Cell-autonomous shift from axial to paraxial mesodermal development in zebrafish floating head mutants. *Development* **121**, 4257-4264.

Henry, C. A. and Amacher, S. L. (2004). Zebrafish slow muscle cell migration induces a wave of fast muscle morphogenesis. *Dev. Cell* **7**, 917-923.

Hernandez-Valladares, M., Kim, T., Kannan, B., Tung, A., Aguda, A. H., Larsson, M., Cooper, J. A. and Robinson, R. C. (2010). Structural characterization of a capping protein interaction motif defines a family of actin filament regulators. *Nat. Struct. Mol. Biol.* **17**, 497-503.

Hirsinger, E., Stellabotte, F., Devoto, S. H. and Westerfield, M. (2004). Hedgehog signaling is required for commitment but not initial induction of slow muscle precursors. *Dev. Biol.* **275**, 143-157.

Ishikura, S., Koshkina, A. and Klip, A. (2008). Small G proteins in insulin action: Rab and Rho families at the crossroads of signal transduction and GLUT4 vesicle traffic. *Acta Physiol. (Oxf.)* **192**, 61-74.

Jia, D., Gomez, T. S., Metlagel, Z., Umetani, J., Otwinowski, Z., Rosen, M. K. and Billadeau, D. D. (2010). WASH and WAVE actin regulators of the Wiskott-Aldrich syndrome protein (WASP) family are controlled by analogous structurally related complexes. *Proc. Natl. Acad. Sci. USA* **107**, 10442-10447.

Lewis, K. E., Concordet, J. P. and Ingham, P. W. (1999). Characterisation of a second patched gene in the zebrafish Danio rerio and the differential response of patched genes to Hedgehog signalling. *Dev. Biol.* **208**, 14-29.

Li, S., Armstrong, C. M., Bertin, N., Ge, H., Milstein, S., Boxem, M., Vidalain, P. O., Han, J. D., Chesneau, A., Hao, T. et al. (2004). A map of the interactome network of the metazoan C. elegans. *Science* **303**, 540-543.

Lu, K., Yin, X., Weng, T., Xi, S., Li, L., Xing, G., Cheng, X., Yang, X., Zhang, L. and He, F. (2008). Targeting WW domains linker of HECT-type ubiquitin ligase Smurf1 for activation by CKIP-1. *Nat. Cell Biol.* **10**, 994-1002.

Mal, T. K., Masutomi, Y., Zheng, L., Nakata, Y., Ohta, H., Nakatani, Y., Kokubo, T. and Ikura, M. (2004). Structural and functional characterization on the interaction of yeast TFIID subunit TAF1 with TATA-binding protein. *J. Mol. Biol.* **339**, 681-693.

Megason, S. G. (2009). In toto imaging of embryogenesis with confocal time-lapse microscopy. *Methods Mol. Biol.* **546**, 317-332.

Moore, C. A., Parkin, C. A., Bidet, Y. and Ingham, P. W. (2007). A role for the Myoblast city homologues Dock1 and Dock5 and the adaptor proteins Crk and Crk-like in zebrafish myoblast fusion. *Development* **134**, 3145-3153.

Nowak, S. J., Nahirney, P. C., Hadjantonakis, A. K. and Baylies, M. K. (2009). Nap1-mediated actin remodeling is essential for mammalian myoblast fusion. *J. Cell Sci.* **122**, 3282-3293.

Odenthal, J., Haffter, P., Vogelsang, E., Brand, M., van Eeden, F. J., Furutani-Seiki, M., Granato, M., Hammerschmidt, M., Heisenberg, C. P., Jiang, Y. J. et al. (1996). Mutations affecting the formation of the notochord in the zebrafish, Danio rerio. *Development* **123**, 103-115.

Olsten, M. E., Canton, D. A., Zhang, C., Walton, P. A. and Litchfield, D. W. (2004). The Pleckstrin homology domain of CK2 interacting protein-1 is required for interactions and recruitment of protein kinase CK2 to the plasma membrane. *J. Biol. Chem.* **279**, 42114-42127.

Pajcini, K. V., Pomerantz, J. H., Alkan, O., Doyonnas, R. and Blau, H. M. (2008). Myoblasts and macrophages share molecular components that contribute to cell-cell fusion. *J. Cell Biol.* **180**, 1005-1019.

Pan, F., Egile, C., Lipkin, T. and Li, R. (2004). ARPC1/Arc40 mediates the interaction of the actin-related protein 2 and 3 complex with Wiskott-Aldrich syndrome protein family activators. *J. Biol. Chem.* **279**, 54629-54636.

Pilot-Storck, F., Chopin, E., Rual, J. F., Baudot, A., Dobrokhotov, P., Robinson-Rechavi, M., Brun, C., Cusick, M. E., Hill, D. E., Schaeffer, L. et al. (2010). Interactome mapping of the phosphatidylinositol 3-kinase-mammalian target of rapamycin pathway identifies deformed epidermal autoregulatory factor-1 as a new glycogen synthase kinase-3 interactor. *Mol. Cell. Proteomics* **9**, 1578-1593.

Pollard, T. D. and Borisy, G. G. (2003). Cellular motility driven by assembly and disassembly of actin filaments. *Cell* **112**, 453-465.

Robinson, R. C., Turbedsky, K., Kaiser, D. A., Marchand, J. B., Higgs, H. N., Choe, S. and Pollard, T. D. (2001). Crystal structure of Arp2/3 complex. *Science* **294**, 1679-1684.

Rochlin, K., Yu, S., Roy, S. and Baylies, M. K. (2010). Myoblast fusion: when it takes more to make one. *Dev. Biol.* **341**, 66-83.

Rual, J. F., Hirozane-Kishikawa, T., Hao, T., Bertin, N., Li, S., Dricot, A., Li, N., Rosenberg, J., Lamesch, P., Vidalain, P. O. et al. (2004). Human ORFeome version 1.1: a platform for reverse proteomics. *Genome Res.* **14 10B**, 2128-2135.

Safi, A., Vandromme, M., Caussanel, S., Valdacci, L., Baas, D., Vidal, M., Brun, G., Schaeffer, L. and Goillot, E. (2004). Role for the pleckstrin homology domain-containing protein CKIP-1 in phosphatidylinositol 3-kinase-regulated muscle differentiation. *Mol. Cell. Biol.* **24**, 1245-1255.

Snow, C. J., Goody, M., Kelly, M. W., Oster, E. C., Jones, R., Khalil, A. and Henry, C. A. (2008). Time-lapse analysis and mathematical characterization elucidate novel mechanisms underlying muscle morphogenesis. *PLoS Genet.* **4**, e1000219.

Srinivas, B. P., Woo, J., Leong, W. Y. and Roy, S. (2007). A conserved molecular pathway mediates myoblast fusion in insects and vertebrates. *Nat. Genet.* **39**, 781-786.

Takeda, S., Minakata, S., Koike, R., Kawahata, I., Narita, A., Kitazawa, M., Ota, M., Yamakuni, T., Maéda, Y. and Nitanai, Y. (2010). Two distinct mechanisms for actin capping protein regulation--steric and allosteric inhibition. *PLoS Biol.* **8**, e1000416.

Thisse, B., Heyer, V., Lux, A., Alunni, V., Degrave, A., Seiliez, I., Kirchner, J., Parkhill, J. P. and Thisse, C. (2004). Spatial and temporal expression of the zebrafish genome by large-scale in situ hybridization screening. *Methods Cell Biol.* **77**, 505-519.

Tokuda, E., Fujita, N., Oh-hara, T., Sato, S., Kurata, A., Katayama, R., Itoh, T., Takenawa, T., Miyazono, K. and Tsuruo, T. (2007). Casein kinase 2-interacting protein-1, a novel Akt pleckstrin homology domain-interacting protein, down-regulates PI3K/Akt signaling and suppresses tumor growth in vivo. *Cancer Res.* **67**, 9666-9676.

Westerfield, M. (2001). *The zebrafish book. A guide for the laboratory use of zebrafish (Danio rerio)*. Eugene, Oregon: University of Oregon Press.

Xi, S., Tie, Y., Lu, K., Zhang, M., Yin, X., Chen, J., Xing, G., Tian, C., Zheng, X., He, F. et al. (2010). N-terminal PH domain and C-terminal auto-inhibitory region of CKIP-1 coordinate to determine its nucleus-plasma membrane shuttling. *FEBS Lett.* **584**, 1223-1230.

Yoon, S., Molloy, M. J., Wu, M. P., Cowan, D. B. and Gussoni, E. (2007). C6ORF32 is upregulated during muscle cell differentiation and induces the formation of cellular filopodia. *Dev. Biol.* **301**, 70-81.

Zalevsky, J., Grigorova, I. and Mullins, R. D. (2001). Activation of the Arp2/3 complex by the Listeria acta protein. Acta binds two actin monomers and three subunits of the Arp2/3 complex. *J. Biol. Chem.* **276**, 3468-3475.

Zhang, L., Xing, G., Tie, Y., Tang, Y., Tian, C., Li, L., Sun, L., Wei, H., Zhu, Y. and He, F. (2005). Role for the pleckstrin homology domain-containing protein CKIP-1 in AP-1 regulation and apoptosis. *EMBO J.* **24**, 766-778.

Zhang, L., Tie, Y., Tian, C., Xing, G., Song, Y., Zhu, Y., Sun, Z. and He, F. (2006). CKIP-1 recruits nuclear ATM partially to the plasma membrane through interaction with ATM. *Cell. Signal.* **18**, 1386-1395.

Zhang, L., Tang, Y., Tie, Y., Tian, C., Wang, J., Dong, Y., Sun, Z. and He, F. (2007). The PH domain containing protein CKIP-1 binds to IFP35 and Nmi and is involved in cytokine signaling. *Cell. Signal.* **19**, 932-944.